Journal of Applied Fluid Mechanics, Vol. 12, No. 3, pp. 987-1000, 2019.
Available online at www.jafmonline.net, ISSN 1735-3572, EISSN 1735-3645.
DOI: 10.29252/jafm.12.03.29101

On Dispersion of a Reactive Solute in a Pulsatile Flow of a Two-Fluid Model

S. Debnath[1], A. K. Saha[1 †], P. G. Siddheshwar[2] and A. K. Roy[1]

[1]*Department of Mathematics, National Institute of Technology, Agartala, Tripura, 799046, India*
[2]*Department of Mathematics, Bangalore University, Bangalore, 560056, India*

†Corresponding Author Email: apusaha_nita@yahoo.co.in

(Received April 11, 2018; accepted November 10, 2018)

ABSTRACT

The present paper is a study on dispersion of reactive solute in an oscillatory flow of a two-fluid, three-layer Casson-Newtonian continuum using Aris-Barton's approach. A two-fluid model of blood flow has been considered, the fluid in the central region is taken to be a Casson fluid (a core of red blood cell suspension) and a peripheral layer of plasma modelled as Newtonian fluid. The governing equations for the velocity distribution have been solved using a perturbation technique, and the effective dispersion coefficient has been evaluated numerically (FDM) by solving the moment equations. Using the Hermite polynomial representation of central moments the axial distribution of mean concentration is determined. The main objective is to look into the impact of yield stress, peripheral layer thickness, irreversible and reversible reaction rate on the dispersion process. The study has significant applications on the transport of species in a blood flow system.

Keywords: Axial-dispersion coefficient; Peripheral layer; Casson fluid; Reaction rate; Two-fluid; Three-layer.

NOMENCLATURE

D	molecular diffusivity
Da	Damköhler number
D_c	apparent dispersion coefficient
e	amplitude of pressure pulsation
j	space index
H_i	Hermite polynomials
i	time index during navigation
r	radial coordinate
Pe	Péclet number
R_p	plug core radius
R_o	central core radius
S_c	concentration of the mobile phase
S_{cs}	concentration of the immobile phase
Sc	Schmidt number
S_{cm}	mean concentration distribution
t	time
ν_2	Skewness
ν_3	Kurtosis
w_{cp}	velocity for plug flow in Casson region
w_c	velocity for shear flow in Casson region
w_n	velocity for shear flow in Newtonian region
z	axial coordinate
τ_c	shear stress of Casson fluid
τ_n	shear stress of Newtonian fluid
τ_y	yield stress
ρ_c	density of Casson fluid
ρ_n	density of Newtonian fluid
μ_c	viscosity of Casson fluid
μ_n	viscosity of Newtonian fluid
α	Womersley frequency parameter
γ	peripheral layer thickness
δ	Dirac delta function
Γ	irreversible reaction rate
Ω	phase exchange rate
μ_k	k^{th} order central moment

1. INTRODUCTION

Hydrodynamic dispersion studies concern the rate of broadening of reactive/nonreactive solute in shear flow, and it depends upon the cross-sectional geometry, discharge velocity, and diffusion coefficient. The other influences on dispersion are flow unsteadiness, chemical reactions, boundary irregularities and such other effects observed in the physiological or extra-corporeal context. In view of its extensive applications in biomedical engineering, physiological fluid dynamics, environmental science and allied fields, the problem of hydrodynamic dispersion of solute in solvent flowing through various conduits has been broadly studied during the last several decades.

Taylor (1953) has initiated the study, investigated the dispersion of a passive solute in a viscous fluid flow through a narrow pipe under steady laminar condition due to the simultaneous action of molecular diffusion and variation of the velocity over the cross-section. Aris (1956) considered longitudinal diffusion to broaden Taylor's hypothesis and built up a technique, 'method of moments' to examine the behaviour of the second-order central moment. But, these two approaches are valid for large time only. Further, Barton (1983) resolved the technical difficulties of Aris's method of moments which is true for all time and is known as Aris-Barton's method of moments.

The transport models exist in the literature, discussing dispersion phenomena in diverse situations. Because of the existence of conductive walls in lungs and blood vessels, it is imperative to discuss the dispersion process take into account the wall property while understanding the indicator dilution technique and other mechanisms in the bronchial region. Considering the absorbing boundary wall reaction, Balasubramanian, Jayaraman, and Iyengar (1997) investigated the dispersion in a curved tube using Taylor's analysis. In an unsteady channel flow, the connection between absorption and the longitudinal dispersion was uncovered by Mondal and Mazumder (2005), utilizing Aris-Barton technique. Using generalized dispersion technique, Sankarasubramanian and Gill (1973) explored dispersion in laminar flows in the presence of first-order reaction at the tube boundary. In few cases flow through the annular tube (Sarkar and Jayaraman (2004), Mazumder and Mondal (2005)) were likewise considered, and also discussed the applicability to a catheterized artery. Transport due to convection and diffusion in a thin (or long) curved (for Newtonian fluid) and circular pipe (for Micropolar fluid) were considered by Marušic-Paloka and Pažanin (2011), and Pažanin (2013) under catalytic wall reaction. Considering a curved channel, Rosencrans (1997) has investigated the effect of curvature on the Taylor dispersion processes. It is found that the effective diffusion is reduced by curvature characteristics. By extending the homogenization technique, Wu and Chen (2014) studied the transverse variation of concentration for the scalar transport along a straight pipe. In a recent work, Roy, Saha, and Debnath (2017), discusses the dispersion of reactive solute released in an unsteady flow between two coaxial cylinders under the presence of first-order reaction in bulk flow.

Of late, dispersion in non-Newtonian fluids has been getting more attention due to its assorted applications in biochemical processing, cardiovascular system, polymer processing, etc. Specifically, in blood flows, species are transmitted as an outcome of diffusive and convective mechanisms. Following the dispersion model of Taylor-Aris, Sharp (1993) investigated the dispersion phenomena in Bingham, Casson, and Power Law fluids flow through conduits, viz., parallel plates and circular tube respectively. Using generalized dispersion technique, the dispersion of a solute in a Casson fluid flowing through pipe and channel was examined by Dash, Jayaraman, and Mehta (2000) who has discussed its utilization in blood flow and established a significant influence of yield stress on the rate of dispersion. Siddheshwar and Manjunath (2000), and Siddheshwar and Markande (1999) were investigated dispersion in plane and Hagen-Poiseuille flows of a Micropolar fluid. Subsequently, Nagarani, Sarojamma, and Jayaraman (2004) considered the effect of boundary absorption on dispersion in such flows of a Casson fluid.

In the above investigations, some of the authors clarified the effectiveness of longitudinal dispersion on blood streams, treating blood as a Newtonian or non-Newtonian fluid depending on the value of shear rate. For the lesser shear rate, experimental results (Charm and Kurland (1965), Blair (1959)) show that Casson fluid model can be suitable to describe the behaviour of blood flow through smaller arteries, with hematocrits, anticoagulants, temperature and other factors included. Further, while blood flows through micro blood vessels, Bugliarello and Sevilla (1970), and Cokelet (1972) has experimentally reported the presence of the peripheral layer of plasma (Newtonian fluid) and a core region of suspension of all the erythrocytes as a non-Newtonian fluid. Thus, in realizing the actual nature of blood streams in micro vessels, it will be more realistic to consider two fluid nature of blood stream rather than a single fluid, where the non-Newtonian property of the core region is represented by Casson model, and the Newtonian fluid represents the plasma layer.

Irreversible and reversible reactions are found to be natural in the human body (especially in blood flow), e.g. (i) the procoagulant subsystem of blood clotting consists of a series of irreversible chemical reactions; (ii) as blood passes through the alveoli of the lungs, hemoglobin molecules pick up oxygen which is then released as the blood travels to other parts of the body. This loading and unloading of oxygen by the blood are similar to a reversible reaction. The effect of reversible phase exchange between the flowing gas in the lumen and the stationary bronchial wall tissue has been studied by Davidson and Schroter (1983). Using homogenization method, Ng (2006) studied the influence of reversible and irreversible reactions on the transport process when fluid flows through a pipe and the same has also been studied by

Paul and Mazumder (2009) considering the annularity of the pipe. Further, an analysis of dispersion under Poiseuille and Couette flow has been done by Debnath, Paul, and Roy (2018) where both the reversible and irreversible reactions exist at the inner wall of the annulus. In view of literature, the studies on the combined effect of reversible and irreversible reactions on dispersion have been mostly assumed in Newtonian fluids, though there is hardly any work which has considered the same for single-fluid Casson model or two-fluid, three-layer models. In the recent work of authors (Debnath, Saha, Mazumder, and Roy (2017b), Debnath, Saha, and Roy (2017), Debnath, Saha, Mazumder, and Roy (2017a)), the effect of interphase mass transfer on the transport coefficients discussed for a two-fluid, three-layer model of Casson-Newtonian continuum under steady and pulsatile nature of the stream. This work incorporates the flow oscillation, two-fluid blood model (solvent in the core and peripheral regions are assumed to be Casson and Newtonian fluid), two kinds of reactions are present at the boundary: reversible (phase exchange) and irreversible (wall absorption) reactions. Thus, the present study is an attempt to bring in as many physiological effects as possible in the blood flow analysis through a rigid artery.

2. THE PROBLEM UNDER CONSIDERATION

We consider a unidirectional axisymmetric flow of a three-layer fluid through a cylindrical pipe (or rigid arteries) of radius $\bar{R}$. Figure 1 depicts the flow geometry for the present model. A cylindrical coordinate system is considered where $\bar{z}$ and $\bar{r}$ represents the axial and radial coordinates respectively (the bar signifies that they are dimensional). The problem is fixed under the following considerations:

(i) Blood is represented as a three-layer fluid with the core of a red blood cell suspension enveloped by a peripheral layer of plasma. For characterizing the blood in the core and peripheral region are described by Casson and Newtonian model respectively.

(ii) The imposed outward periodic pressure gradient has been taken for characterizing the unsteadiness in species transport and is given by:

$$-\frac{\partial \bar{p}}{\partial \bar{z}} = A_0 + A_1 \sin(\omega_p \bar{t}), \tag{1}$$

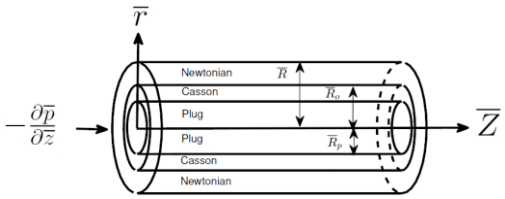

Fig. 1. Three-layer Casson-Newtonian continuum.

where $\bar{p}$ is the pressure, A_0 and A_1 are the steady and fluctuating components of the pressure gradient, ω_p is the pulse frequency, and $\bar{t}$ is time.

(iii) The low Reynolds number flow is supposed to be laminar, axisymmetric, incompressible and in fully developed region streams are directed only in the axial direction as the system in the axial direction is infinitely extended. Let, the axial component of velocities for Casson and Newtonian fluid is $\bar{w}_c(\bar{r},\bar{t})$ and $\bar{w}_n(\bar{r},\bar{t})$ which satisfies the momentum equation in the axial direction as:

$$\bar{\rho}_c \frac{\partial \bar{w}_c}{\partial \bar{t}} = -\frac{\partial \bar{p}}{\partial \bar{z}} - \frac{1}{\bar{r}} \frac{\partial (\bar{r}\,\bar{\tau}_c)}{\partial \bar{r}} \qquad 0 \le \bar{r} \le \bar{R}_o, \tag{2}$$

$$\bar{\rho}_n \frac{\partial \bar{w}_n}{\partial \bar{t}} = -\frac{\partial \bar{p}}{\partial \bar{z}} - \frac{1}{\bar{r}} \frac{\partial (\bar{r}\,\bar{\tau}_n)}{\partial \bar{r}} \qquad \bar{R}_o \le \bar{r} \le \bar{R}, \tag{3}$$

here $\bar{\tau}_c$ and $\bar{\tau}_n$ are the shear stress of Casson and Newtonian fluids, also $\bar{\rho}_c$ and $\bar{\rho}_n$ are the densities of the respective fluids. The quantity $\bar{R}_o$ is the ratio of the central core radius to the normal pipe radius. The Casson constitutive equation is a non-linear relation between shear stress and shear rate (Aroesty and Gross (1972)), and that of a Newtonian fluid is a simple linear one. Hence the time-dependent, unidirectional flows in different regions of the system are governed by:

$$\left.\begin{array}{ll} \dfrac{\partial \bar{w}_c}{\partial \bar{r}} = 0 & \text{if } \bar{\tau}_c \le \bar{\tau}_y \text{ for } 0 \le \bar{r} \le \bar{R}_p \\ \bar{\tau}_c^{\frac{1}{2}} = \bar{\tau}_y^{\frac{1}{2}} + (-\bar{\mu}_c \dfrac{\partial \bar{w}_c}{\partial \bar{r}})^{\frac{1}{2}} & \text{if } \bar{\tau}_c \ge \bar{\tau}_y \text{ for } \bar{R}_p \le \bar{r} \le \bar{R}_o \\ \bar{\tau}_n = -\bar{\mu}_n \dfrac{\partial \bar{w}_n}{\partial \bar{r}} & \text{if } \bar{\tau}_y = 0 \text{ for } \bar{R}_o \le \bar{r} \le \bar{R} \end{array}\right\}, \tag{4}$$

with the boundary conditions

$$\left.\begin{array}{lll} \bar{\tau}_c \text{ is finite, and } \dfrac{\partial \bar{w}_c}{\partial \bar{r}} = 0 & \text{at} & \bar{r} = 0 \\ \bar{\tau}_c = \bar{\tau}_n, \text{ and } \bar{w}_c = \bar{w}_n & \text{at} & \bar{r} = \bar{R}_o \\ \bar{w}_n = 0 & \text{at} & \bar{r} = \bar{R} \end{array}\right\}, \tag{5}$$

where $\bar{\tau}_y$ and $\bar{R}_p$ are the yield stress and plug core radius. The quantity $\bar{\mu}_c$ and $\bar{\mu}_n$ are the viscosity for Casson and Newtonian fluids. In Eq. (4), the velocity gradient will be zero if $\bar{\tau}_c \le \bar{\tau}_y$, implying the existence of plug flow region.

We suppose that blood is flowing through an artery and some finite amount of chemical species is injected into the flow. We assume that the species is completely miscible with the flowing fluid and will undergo two kinds of reaction at the boundary: reversible phase exchange with the wall material and irreversible absorption at the wall. Due to the reaction considered above, it is realized that some of species segment adheres to the tube

wall and rest of the species move with the streaming fluid. Hence to recognize the type of chemical substance, two phases are considered in the modelling of species: mobile phase and immobile phase. Species that flows with fluid is known as mobile phase, and that which is fixed at the wall is known as immobile phase.

Let the concentration of the mobile phase be $\bar{S}_c$, and the concentration of the immobile or stationary phase be $\bar{S}_{cs}$. In equilibrium, they can be represented by a ratio, viz., partition coefficient as: $\frac{\bar{S}_{cs}}{\bar{S}_c} = \bar{\Omega}$ (constant).

In general, when equilibrium is not achieved, the following first-order kinetics describes the exchange of the two phases:

$$\frac{\partial \bar{S}_{cs}}{\partial \bar{t}} = K(\bar{\Omega}\bar{S}_c - \bar{S}_{cs}) \tag{6}$$

where K is a constant represents the rate of the reversible reaction.

The convection-diffusion equation for the present problem is:

$$\frac{\partial \bar{S}_c}{\partial \bar{t}} + \bar{w}(\bar{r},\bar{t})\frac{\partial \bar{S}_c}{\partial \bar{z}} = D\frac{\partial^2 \bar{S}_c}{\partial \bar{z}^{-2}} + \frac{D}{\bar{r}}\frac{\partial}{\partial \bar{r}}\left(\bar{r}\frac{\partial \bar{S}_c}{\partial \bar{r}}\right), \tag{7}$$

here D is the constant molecular diffusivity.

The initial and boundary conditions for solving the transport Eq. (7) are

$$\left.\begin{aligned} \bar{S}_c(0,\bar{r},\bar{z}) &= \bar{S}_{c0}\, X(\bar{r})\phi(\bar{z}), \quad (0<\bar{r}<\bar{R}) \\ \bar{S}_{c0} &= \frac{M}{\pi \bar{R}^3} \\ \phi(\bar{z}) &= \frac{\bar{R}\,\delta(\bar{z})}{d^2} \\ X(\bar{r}) &= \begin{cases} 1 & \text{for } 0 \le \bar{r} \le d\bar{R} \\ 0 & \text{for } d\bar{R} < \bar{r} \le \bar{R} \end{cases} \end{aligned}\right\}, \tag{8}$$

$$\bar{S}_c = 0 \text{ as } \bar{z} \to \pm\infty \tag{9}$$

for a finite extent of axial distribution

$$\frac{\partial \bar{S}_c}{\partial \bar{r}} = 0 \quad \text{at} \quad \bar{r} = 0, \tag{10}$$

$$-D\frac{\partial \bar{S}_c}{\partial \bar{r}} - \bar{\Gamma}\bar{S}_c = \frac{\partial \bar{S}_{cs}}{\partial \bar{t}} = K(\bar{\Omega}\,\bar{S}_c - \bar{S}_{cs}) \text{ at } \bar{r} = \bar{R}, \tag{11}$$

where $X(\bar{r})$ and $\delta(\bar{z})$ refer to a function of $\bar{r}$ and the Dirac delta function. $\bar{S}_{c0}$ is the concentration of solute mass uniformly introduced over the cross-section of a circle of radius $d\bar{R}$ at time zero. Here $'d'$ is the ratio of the radius of the cylinder containing solute to that of the entire tube. If $d = 1$, initially the concentration cloud occupies the entire cross-section of the pipe.

Following dimensionless quantities are assumed for the present problem:

$$\left.\begin{aligned} S_c &= \frac{\bar{S}_c}{\bar{S}_{c0}},\ S_{cs} = \frac{\bar{S}_{cs}}{\bar{R}\,\bar{S}_{c0}},\ w_c = \frac{\bar{w}_c}{w_{0c}},\ w_n = \frac{\bar{w}_n}{w_{0n}}, \\ w_{0c} &= -\frac{\bar{R}^2}{4\bar{\mu}_c}\frac{d\bar{p}}{d\bar{z}},\ w_{0n} = -\frac{\bar{R}^2}{4\bar{\mu}_n}\frac{d\bar{p}}{d\bar{z}},\ r = \frac{\bar{r}}{\bar{R}}, \\ R_0 &= \frac{\bar{R}_o}{\bar{R}},\ R_p = \frac{\bar{R}_p}{\bar{R}},\ z = \frac{D\bar{z}}{\bar{R}^2 w_0},\ t = \frac{D\bar{t}}{\bar{R}^2}, \\ \tau_c &= \frac{\bar{\tau}_c}{\bar{\mu}_c(\frac{w_{0c}}{\bar{R}})},\ \tau_n = \frac{\bar{\tau}_n}{\bar{\mu}_n(\frac{w_{0n}}{\bar{R}})},\ \tau_y = \frac{\bar{\tau}_y}{\bar{\mu}_c(\frac{w_{0c}}{\bar{R}})}, \\ Pe &= \frac{w_0\bar{R}}{D},\ Sc = \frac{\nu}{D},\ Da = \frac{K\bar{R}^2}{D},\ \Gamma = \frac{\bar{\Gamma}\bar{R}}{D}, \\ \Omega &= \frac{\bar{\Omega}}{\bar{R}} \end{aligned}\right\} \tag{12}$$

here w_0 denotes the time-averaged velocity in the axial direction. Pe is the Pèclet number, defined as the ratio of advection rate to the diffusion rate of species transport. Sc is the Schmidt number, describes the relation among viscous diffusion to the molecular diffusion.

Substituting the above dimensionless quantities in Eqs. (7) - (11) may be rewritten as :

$$\frac{\partial S_c}{\partial t} + w(r,t)\frac{\partial S_c}{\partial z} = \frac{1}{r}\frac{\partial}{\partial r}\left(r\frac{\partial S_c}{\partial r}\right) + \frac{1}{Pe^2}\frac{\partial^2 S_c}{\partial z^2} \tag{13}$$

$$\left.\begin{aligned} S_c(0,r,z) &= X(r)\phi(z), \quad (0<r<1) \\ \phi(z) &= \frac{\delta(z)}{d^2\, Pe} \\ X(r) &= \begin{cases} 1 & \text{for } 0 \le r \le d \\ 0 & \text{for } d < r \le 1 \end{cases} \end{aligned}\right\}, \tag{14}$$

$$S_c = 0 \quad \text{as} \quad z \to \pm\infty, \tag{15}$$

$$\frac{\partial S_c}{\partial r} = 0 \quad \text{at} \quad r = 0, \tag{16}$$

$$-\frac{\partial S_c}{\partial r} - \Gamma S_c = Da(\Omega S_c - S_{cs}) \quad \text{at} \quad r = 1, \tag{17}$$

The significance of the parameters Da , Γ and Ω representing the heterogeneous reactions at the boundary of the tube is noted in Table 1.

The quantity S_{cn} (concentration of the immobile phase) mentioned in Eq. (17) is governed by non-dimensioning Eq. (6) as:

$$\frac{\partial}{\partial t}S_{cs}(t,z) = Da[\Omega\, S_c(t,1,z) - S_{cs}(t,z)], \quad \text{with } S_{cs}(0,z) = 0. \tag{18}$$

Table 1 Physical significance of reactions parameter

Parameter	Name	Physical significance
Da	Damkhöler number	Represent the kinetics of the phase exchange; if $Da \gg 1$, then the reaction rate is much greater than the diffusion rate.
Γ	Absorption parameter	Represents the rate of solute of loss; if $\Gamma \gg 1$, then huge amount of mass is depleted in a short time.
Ω	Phase partition ratio	Represents retention if $\Omega \ll 1$, then partition happens more readily between the phases and the opposite is true for $\Omega \gg 1$.

3. VELOCITY DISTRIBUTION

Using the above dimensionless quantities to the Eqs. (1) - (5) are:

$$\varepsilon \frac{\partial w_c}{\partial t} = 4p(t) - \frac{1}{r}\frac{\partial (r\tau_c)}{\partial r} \qquad 0 \le r \le R_o, \tag{19}$$

$$\varepsilon \frac{\partial w_n}{\partial t} = 4p(t) - \frac{1}{r}\frac{\partial (r\tau_n)}{\partial r} \qquad R_o \le r \le 1, \tag{20}$$

$$\left.\begin{aligned} &\frac{\partial w_c}{\partial r} = 0 && \text{if } \tau_c \le \tau_y \text{ for } 0 \le r \le R_p \\ &\tau_c^{\frac{1}{2}} = \tau_y^{\frac{1}{2}} + (-\frac{\partial w_c}{\partial r})^{\frac{1}{2}} && \text{if } \tau_c \ge \tau_y \text{ for } R_p \le r \le R_o \\ &\tau_n = -\frac{\partial w_n}{\partial r} && \text{if } \tau_y = 0 \text{ for } R_o \le r \le 1 \end{aligned}\right\}, \tag{21}$$

$$\left.\begin{aligned} &\tau_c \text{ is finite, and } \frac{\partial w_c}{\partial r} = 0 && \text{at } r = 0, \\ &\tau_c = \tau_n, \text{ and } w_c = w_n && \text{at } r = R_o, \\ &w_n = 0 && \text{at } r = 1, \end{aligned}\right\}. \tag{22}$$

Here $p(t) = (1 + e\sin(\alpha^2 Sc\ t))$, $e = \frac{A_1}{A_0}$ is the amplitude of the fluctuating pressure component, α is the Womersley frequency parameter. The analytical solution for the velocity distribution may not be possible here due to the non-linear coupled relations among Eqs. (19) - (21). Thus to solve the same we have followed the perturbation technique with perturbation parameter as ($\varepsilon = \frac{1}{Sc}$, inverse of Schmidt number). While blood flows through small artery (Caro, Pedley, Schroter, and Seed (1978)), the Schmidt number (Sc) is supposed to be very high ($O(10^3)$) hence, ε is so small. The flow velocity in small blood vessels and coronary artery can be portrayed by considering the Womersley number to be small. Now, we suppose a regular perturbation solution of the form:

$$\left.\begin{aligned} w_c(r,t) &= w_{0c}(r,t) + \epsilon\, w_{1c}(r,t) + \cdots, \\ w_n(r,t) &= w_{0n}(r,t) + \epsilon\, w_{1n}(r,t) + \cdots, \\ \tau_c(r,t) &= \tau_{0c}(r,t) + \epsilon\, \tau_{1c}(r,t) + \cdots, \\ \tau_n(r,t) &= \tau_{0n}(r,t) + \epsilon\, \tau_{1n}(r,t) + \cdots, \end{aligned}\right\}. \tag{23}$$

Utilizing Eq. (23) in Eqs. (19) - (22), we get

Zeroth Order Terms :

$$\frac{\partial}{\partial r}(r\tau_{0c}) = 4p(t)r, \tag{24}$$

$$-\frac{\partial w_{0c}}{\partial r} = \tau_{0c} + \tau_y - 2\tau_y^{\frac{1}{2}}\tau_{0c}^{\frac{1}{2}}, \tag{25}$$

$$\frac{\partial}{\partial r}(r\tau_{0n}) = 4p(t)r, \tag{26}$$

$$\tau_{0n} = -\frac{\partial w_{0n}}{\partial r}, \tag{27}$$

First Order Terms :

$$\frac{\partial w_{0c}}{\partial t} = -\frac{1}{r}\frac{\partial}{\partial r}(r\tau_{1c}), \tag{28}$$

$$-\frac{\partial w_{1c}}{\partial r} = \tau_{1c}\left(1 - \sqrt{\frac{\tau_y}{\tau_{0c}}}\right) \tag{29}$$

$$\frac{\partial w_{0n}}{\partial t} = -\frac{1}{r}\frac{\partial}{\partial r}(r\tau_{1n}), \tag{30}$$

$$\tau_{1n} = -\frac{\partial w_{1n}}{\partial r}. \tag{31}$$

The boundary conditions for solving Eqs. (24) - (31) are:

$$\left.\begin{aligned} &\tau_{0c} \text{ and } \tau_{1c} \text{ are finite and } \frac{\partial w_{0c}}{\partial r} = 0, \frac{\partial w_{1c}}{\partial r} = 0 && \text{at } r = 0, \\ &\tau_{0c} = \tau_{0n},\ \tau_{1c} = \tau_{1n},\ w_{0c} = w_{0n},\ w_{1c} = w_{1n} && \text{at } r = R_o, \\ &w_{0n} = w_{1n} = 0 && \text{at } r = 1, \end{aligned}\right\}. \tag{32}$$

Solving the BVP of Eqs. (24) – (32), we get

$$\tau_{0c} = 2p(t)r, \tag{33}$$

$$w_{0c}(r,t)=p(t)\left[(1-R_0^2)+R_0^2\left\{1-\xi_1^2-\frac{4\sqrt{2}}{3}\xi_2^{\frac{1}{2}}\left(1-\xi_1^{\frac{3}{2}}\right)+\xi_2(1-\xi_1)\right\}\right], \qquad R_p \le r \le R_o \tag{34}$$

$$\tau_{0n}=2p(t)r, \tag{35}$$

$$w_{0n}(r,t)=p(t)(1-r^2), \qquad R_o \le r \le 1 \tag{36}$$

$$\tau_{1c}=-p'(t)\left[\frac{r}{2}(1-R_o^2)+R_o^2\left\{\frac{r}{2}-\frac{r^3}{4R_o^2}-\frac{2\sqrt{2}}{3}\sqrt{\frac{\tau_y}{R_o\ p(t)}}\left(\frac{r}{2}-\frac{2}{7}\frac{r^{5/2}}{R_o^{3/2}}\right)\right\}\right], \tag{37}$$

$$\begin{aligned}w_{1c}(r,t)=\frac{p'(t)}{16}\Big[&R_o\log(R_0)\left\{8R_o(1-R_0^2)+R_o^3\left(4-\frac{16\sqrt{(2\xi_2)}}{7}\right)\right\}-R_o^4+4R_o^2-3\\&-4R_o^2(2-R_o^2)\log(R_o)-4R_o^2(1-R_o^2)(1-\xi_1^2)\\&-R_o^4\left\{3-\frac{32\sqrt{2\xi_2}}{3}\left(\frac{33}{196}-\frac{\xi_1^2}{4}+\frac{4}{49}\xi_1^{\frac{7}{2}}\right)-4\xi_1^2+\xi_1^4\right\}+\frac{16}{3\sqrt{2}}R_o^2(1-R_o^2)\left(1-\xi_1^{\frac{3}{2}}\right)\\&+\frac{16R_o^4}{\sqrt{2}}\sqrt{\xi_2}\left\{\frac{11}{42}-\frac{2\sqrt{2}}{3}\xi_1^{\frac{1}{2}}\left(\frac{5}{21}-\frac{1}{3}\xi_1^{\frac{3}{2}}+\frac{2}{21}\xi_1^3\right)-\frac{1}{3}\xi_1^{\frac{3}{2}}+\frac{1}{14}\xi_1^{\frac{7}{2}}\right\}\Big],\end{aligned} \qquad R_p \le r \le R_o \tag{38}$$

$$\tau_{1n}=-p'(t)\left[\frac{r}{2}-\frac{r^3}{4}-\frac{R_o^2}{2r}+\frac{R_o^4}{4r}+\frac{R_o}{r}\left\{\frac{1}{2}R_0(1-R_o^2)+R_o^3\left(\frac{1}{4}-\frac{1}{7}\sqrt{\frac{2\tau_y}{p(t)R_o}}\right)\right\}\right] \tag{39}$$

$$\begin{aligned}w_{1n}(r,t)=\frac{p'(t)}{16}\Big[&R_o\log(r)\left\{8R_o(1-R_0^2)+R_o^3\left(4-\frac{16\sqrt{(2\xi_2)}}{7}\right)\right\}-r^4+4r^2\\&-3-4R_0^2(2-R_0^2)\log(r)\Big],\end{aligned} \qquad R_o \le r \le 1. \tag{40}$$

Substituting the value $r=R_p$ in Eqs. (34) and (38) we can get the expressions for w_{op} and w_{1p} as:

$$w_{0p}(r,t)=p(t)\left[(1-R_0^2)+R_0^2\left\{1-\xi_2^2-\frac{4\sqrt{2}}{3}\xi_2^{\frac{1}{2}}\left(1-\xi_2^{\frac{3}{2}}\right)+\xi_2(1-\xi_2)\right\}\right], \qquad 0 \le r \le R_p \tag{41}$$

$$\begin{aligned}w_{1p}(r,t)=\frac{p'(t)}{16}\Big[&R_o\log(R_0)\left\{8R_o(1-R_0^2)+R_o^3\left(4-\frac{16\sqrt{(2\xi_2)}}{7}\right)\right\}-R_o^4+4R_o^2-3\\&-4R_o^2(2-R_o^2)\log(R_o)-4R_o^2(1-R_o^2)(1-\xi_2^2)\\&-R_o^4\left\{3-\frac{32\sqrt{2\xi_2}}{3}\left(\frac{33}{196}-\frac{\xi_2^2}{4}+\frac{4}{49}\xi_2^{\frac{7}{2}}\right)-4\xi_2^2+\xi_2^4\right\}+\frac{16}{3\sqrt{2}}R_o^2(1-R_o^2)\left(1-\xi_2^{\frac{3}{2}}\right)\\&+\frac{16R_o^4}{\sqrt{2}}\sqrt{\xi_2}\left\{\frac{11}{42}-\frac{2\sqrt{2}}{3}\xi_2^{\frac{1}{2}}\left(\frac{5}{21}-\frac{1}{3}\xi_2^{\frac{3}{2}}+\frac{2}{21}\xi_2^3\right)-\frac{1}{3}\xi_2^{\frac{3}{2}}+\frac{1}{14}\xi_2^{\frac{7}{2}}\right\}\Big],\end{aligned} \qquad 0 \le r \le R_p, \tag{42}$$

where $\xi_1=\frac{r}{R_o}$, $\xi_2=\frac{R_p}{R_o}$, and $R_p=\frac{\tau_y}{p(t)}$ is the plug core radius. Considering the first two-terms of the perturbation series the solution of velocity distribution in their respective layers are as:

$$\left.\begin{aligned}w_{cp}(r,t)&=w_{0p}+\varepsilon w_{1p} \quad \text{for} \quad 0 \le r \le R_p,\\ w_c(r,t)&=w_{0c}+\varepsilon w_{1c} \quad \text{for} \quad R_p \le r \le R_o,\\ w_n(r,t)&=w_{0n}+\varepsilon w_{1n} \quad \text{for} \quad R_o \le r \le 1,\end{aligned}\right\}. \tag{43}$$

In Eq. (43), w_c and w_n are the velocities for shear flow in the Casson and Newtonian regions whereas w_{cp} is the constant velocity for plug flow region. The peripheral layer thickness can be approximated by R_o and is defined as $\gamma(=[1-R_o])$. Thus the present three-layer model will be reduced to a single-fluid Casson model if one consider $R_o=1$ or $\gamma=0$.

4. MOMENT EQUATIONS

The k^{th} moment of concentration distribution for the mobile phase can be defined, following Aris (1956), as

$$S_c^{(k)}(t,r)=\int_{-\infty}^{+\infty} z^k S_c(t,r,z)dz \tag{44}$$

and likewise for the immobile phase we may assume:

$$S_{cs}^{(k)}(t)=\int_{-\infty}^{+\infty} z^k S_{cs}(t,z)dz. \tag{45}$$

Using Eqs. (44) and (45), the Eqs. (13) - (17) can be rewritten in the form of $S_c^{(k)}$ and $S_{cs}^{(k)}$ as:

$$\frac{\partial S_c^{(k)}}{\partial t}-\frac{1}{r}\frac{\partial}{\partial r}\left(r\frac{\partial S_c^{(k)}}{\partial r}\right)=kw(r,t)S_c^{(k-1)} +\frac{1}{Pe^2}k(k-1)S_c^{(k-2)}, \tag{46}$$

with

$$\left.\begin{aligned} &S_c^{(k)}(0,r)=\begin{cases}\dfrac{X(r)}{d^2Pe} & \text{for } k=0\\ 0 & \text{for } k>0\end{cases}\\ &\frac{\partial S_c^{(k)}}{\partial r}=0 \quad \text{at} \quad r=0,\\ &-\frac{\partial S_c^{(k)}}{\partial r}-\Gamma S_c^{(k)}=Da\left[\Omega S_c^{(k)}-S_{cs}^{(k)}\right] \quad \text{at} \quad r=1 \end{aligned}\right\}. \tag{47}$$

In the immobile phase the equation for the moments of the mass distribution is

$$\frac{d}{dt}S_{cs}^{(k)}=Da\left[\Omega S_c^{(k)}(t,1)-S_{cs}^{(k)}\right], \quad \text{with initial condition } S_{cs}^{(k)}(0)=0. \tag{48}$$

Using integral moment, the cross-sectional mean concentration for the mobile phase can be defined as:

$$\left\langle S_c^{(k)}(t)\right\rangle=2\int_0^1 r\,S_c^{(k)}(t,r)dr, \tag{49}$$

with this definition, Eqs. (46) and (47) become

$$\frac{d}{dt}\left\langle S_c^{(k)}\right\rangle=2\left[Da\,S_{cs}^{(k)}(t)-(\Gamma+Da\Omega)S_c^{(k)}(t,1)\right] +k\left\langle w(r,t)S_c^{(k-1)}\right\rangle+\frac{1}{Pe^2}k(k-1)\left\langle S_c^{(k-2)}\right\rangle, \tag{50}$$

$$\left\langle S_c^{(k)}(0)\right\rangle=\left.\begin{aligned}&\frac{1}{Pe} \quad \text{for } k=0\\ &0 \quad \text{for } k>0\end{aligned}\right\}. \tag{51}$$

The k^{th} order central moment about mean of the concentration distribution can be defined as

$$\mu_k(t)=\frac{\int_0^1\int_0^{2\pi}\int_{-\infty}^{+\infty}r(z-z_g)^k S_c\,dr\,d\theta\,dz}{\int_0^1\int_0^{2\pi}\int_{-\infty}^{+\infty}rS_c\,dr\,d\theta\,dz}, \tag{52}$$

where

$$z_g=\frac{\iiint z\,S_c\,d\nu}{\iiint S_c\,d\nu}=\frac{\left\langle S_c^{(1)}\right\rangle}{\left\langle S_c^{(0)}\right\rangle}$$

represents the 'centroid' or 'first moment' of the solute distribution; $\left\langle S_c^{(0)}\right\rangle$ refers to the entire mass of the chemical species in the flowing stream.

The higher order central moments achieved from Eq. (52) for values of $k=2,3,4,$ are:

$$\left.\begin{aligned}&\mu_2(t)=\frac{\left\langle S_c^{(2)}\right\rangle}{\left\langle S_c^{(0)}\right\rangle}-z_g^{\,2},\\ &\mu_3(t)=\frac{\left\langle S_c^{(3)}\right\rangle}{\left\langle S_c^{(0)}\right\rangle}-3z_g\mu_2-z_g^{\,3},\\ &\mu_4(t)=\frac{\left\langle S_c^{(4)}\right\rangle}{\left\langle S_c^{(0)}\right\rangle}-4z_g\mu_3-6z_g^{\,2}\mu_2-z_g^{\,4},\end{aligned}\right\}. \tag{53}$$

Aris (1956) first discovered the physical significance of these central moments to the dispersion process. The overall behaviour of the slug can be efficiently described by these integral moments. Among them, the dispersion coefficient, D_c can be obtained from the second central moment, μ_2 and is written as:

$$D_c=\frac{1}{2}\frac{d\mu_2}{dt}. \tag{54}$$

The coefficient of Skewness $\nu_2(=\mu_3/\mu_2^{\frac{3}{2}})$ and Kurtosis $\nu_3(=\mu_4/\mu_2^2-3)$ are also imperative as to measure the degree of symmetry and peakedness of the concentration distribution respectively.

5. NUMERICAL SOLUTION OF MOMENT EQUATIONS

In this section, using the finite difference Crank-Nicolson implicit scheme, a numerical solution of the moment Eq. (46) subject to the conditions (47), together with Eq. (48) has been presented for all time dispersion analysis. The solute is supposed to inject uniformly over the cross-section of the pipe. We consider $(M-1)$ parts having same length Δr to divide the whole width of the tube, and they are illustrated by the grid point j along *r*-axis. Thus the general formula can be written as $r_j=(j-1)\times\Delta r$ when Δr is the increment of r. Let, i represents the grid point for time along *t*-axis and Δt be the increment of t, then the general formula for time is also written as $t_i=\Delta t\times(i-1)$. From the above mentioned formulas, it can be realized that the grid

values at pipe's axis ($r=0$) and wall ($r=1$) can be obtained for $j=1$ and M respectively, whereas values at initial time ($t=0$) are found for $i=1$. Let, the discretized values of $S_c^{(k)}$ is denoted by $S_c^{(k)}(i,j)$ at their corresponding grid points. With the use of above discretization technique, the moment equation is now transformed to a set of algebraic equations:

$$P_j S_c^{(k)}(i+1,j+1)+Q_j S_c^{(k)}(i+1,j) +R_j S_c^{(k)}(i+1,j-1)=T_j, \tag{55}$$

where P_j, Q_j, R_j and T_j are the matrix elements.

The discretized form of initial and boundary conditions are:

$$S_c^{(k)}(1,j)=\begin{cases}\dfrac{1}{Pe} & \text{for} \quad k=0\\ 0 & \text{for} \quad k>0\end{cases} \tag{56}$$

$$\left.\begin{array}{l} S_c^{(k)}(i+1,0)=S_c^{(k)}(i+1,2), \\ \text{(axis of pipe), and} \\ S_c^{(k)}(i+1,M+1)=S_c^{(k)}(i+1,M-1) \\ -2\Delta r(\Gamma+Da\Omega)S_c^{(k)}(i+1,M) \\ +2\Delta r\ Da\ S_{cs}^{(k)}(i), \quad \text{(pipe wall)} \end{array}\right\}. \tag{57}$$

Where $S_{cs}^{(k)}(i)$ can be computed from relation:

$$S_{cs}^{(k)}(i+1)=\frac{S_{cs}^{(k)}(i)+Da\ \Delta t\Omega\ S_c^{(k)}(i+1,M)}{1+Da\ \Delta t}, \tag{58}$$

with the initial condition $S_{cs}^{(k)}(1)=0$.

Due to the nature of tridiagonal coefficient matrix in Eq. (55), Thomas algorithm (Anderson, Tannehill, and Pletcher (1984)) has been followed by means of a MATLAB code, with the assistance of Eqs. (56) - (58). Details of the computation are mentioned in below:

Step-1: Time-dependent axial velocity, $w(r,t)$ is calculated first at all grid points using Eq. (43).

Step-2: As $w(r,t)$ is known in its grid points, then, $S_c^{(k)}$ is computed from Eq. (46).

Step-3: From Eq. (48), $S_{cs}^{(k)}$ is computed with the use of $S_c^{(k)}$ obtained from **Step-2**.

Step-4: Finally with the use of required values obtained from **Step-1** to **3** at the corresponding grid points, $\left\langle S_c^{(k)}\right\rangle$ is evaluated from Eq. (49) with the help of Simpson's one-third method.

Numerical calculations have been executed for steady and unsteady velocity profiles with respect to yield stress, peripheral layer thickness, and with various reaction parameters to understand the individual dispersion processes. The present scheme is linearly stable for any finite value of $\Delta t/(\Delta r)^2$, and with the variation of parameters value there is always a satisfactory result for a fixed mesh size ($\Delta t=0.00001,\ \Delta r=1/(M-1)$) and $M=100$ respectively. During the computation, $d=1$, $\Omega=0.5,\ Pe=Sc=10^3,\ \alpha=e=0.5$ are always kept constant. Using the aforementioned space and time discretization parameters an accuracy of 10^{-5} in the results have been confirmed. The dispersion process due to pulsatile nature of stream can be better recognized with the approximation of small time step. The stability and that of the accuracy of the results can be achieved with the consideration of small space discretization.

6. DISTRIBUTIONS OF MEAN CONCENTRATION

Using moments method we did not have the solution for concentration distribution, but those of the first four moments can be useful to find the mean concentration distribution, $S_{cm}(t,z)$ in the axial direction. For that purpose, we use the concept of Hermite polynomial representation for non-Gaussian curves (Mehta, Merson, and McCoy (1974)), as:

$$S_{cm}(t,z)=\left\langle S_c^{(0)}(t)\right\rangle e^{-\chi^2}\sum_{n=0}^{\infty} b_n(t)H_n(\chi), \tag{59}$$

where $\chi=\dfrac{(z-z_g)}{\sqrt{2\mu_2}}$, $z_g=\dfrac{\left\langle S_c^{(1)}\right\rangle}{\left\langle S_c^{(0)}\right\rangle}$ and H_n 's are Hermite polynomials that satisfy the recurrence relation with $H_0(\chi)=1$:

$$H_{n+1}(\chi)=2\chi H_n(\chi)-2nH_{n-1}(\chi),\quad n=0,1,2,....$$

The coefficients b_n 's are:

$$b_0=\frac{1}{\sqrt{2\pi\mu_2}},\ b_1=b_2=0,\ b_3=\frac{\sqrt{2}b_0\nu_2}{24},\ b_4=\frac{b_0\nu_3}{96}.$$

With the use of central moments documented in Eq. (53), we can now calculate $S_{cm}(t,z)$ axially from Eq. (59) at any given location and time.

7. RESULTS AND DISCUSSION

This study considers the effect of peripheral layer thickness on dispersion of reactive substances in a two-fluid, three-layer Casson-Newtonian continuum flowing through a narrow pipe when reversible and irreversible reactions exist at the boundary. The rheological parameter (or yield stress) is chosen to be small ($0.04\ dyn/cm^2$) as suggested by McDonald (1974) for blood flow in small diameter arteries. An attempt has been made to mathematically model the blood flow situation through a rigid artery. In this

work, the method of moments has been followed to estimate the dispersion coefficient numerically. The proposed numerical technique is validated by Case-I to III, as:

Case-I: $\gamma = 0,\ e = 0,\ Da = 0$ and $R_p = 0.0,$ 0.02, 0.04, 0.06, 0.08, 0.1, 0.2; correspond to the study of dispersion in the presence of interphase mass transfer when the driving force has only a constant pressure gradient. Figure 2 is the plot of dispersion coefficient vs irreversible absorption parameter (Γ), which completely concurs with the result obtained by Sankarasubramanian and Gill (1973) when $R_p = 0.0$ (Newtonian fluid) and also satisfies the results for Nagarani, Sarojamma, and Jayaraman (2004) for non-zero choices of R_p (Casson fluid). It is important to specify here that Sankarasubramanian and Gill (1973) and Nagarani, Sarojamma, and Jayaraman (2004) used normalization scales different than that used in our work and so, in some cases, the scalar value of dispersion coefficients differ but the tenet, however, is similar to ours.

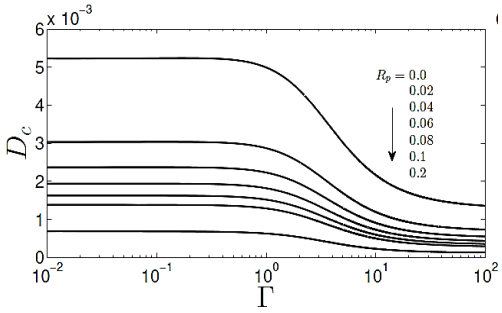

Fig. 2. Variation of dispersion coefficient (D_c) with absorption parameter (Γ) for various values of plug radius (R_p) for the case when $\gamma = 0,\ Da = 0,$ and $e = 0.$

Case-II: The variation of D_c with time is shown in Fig. 3(a) by considering $\gamma = 0,\ Da = 0,$ and $R_p = 0$ under periodic pressure gradient ($\alpha = e = 0.5$), which satisfies the qualitative nature of the results in Fig. 7 of Mazumder and Das (1992).

Case-III: For the parameters values described in Fig. 3(b), the combined effect of reversible phase exchange and irreversible absorption can be perceived under steady Newtonian fluid flow situation (i.e., $\gamma = R_p = e = 0$), a result has been noticed previously by Lau and Ng (2007). [Fig. 3(b) become like Fig. 1 of Lau and Ng (2007)].

The time evaluation of D_c for different values of the reaction parameters has been plotted in Figs. 4 and 5 for small and large time intervals. During this study, the small and large time intervals are intended within the range of [0 -0.08] and [0.42 - 0.5] respectively. Figs. 4(a, b) demonstrate the effect of phase exchange rate while Figs. 5(a, b) demonstrate the effect of absorption parameter at the pipe boundary on D_c. From Fig. 4(a), it can be easily

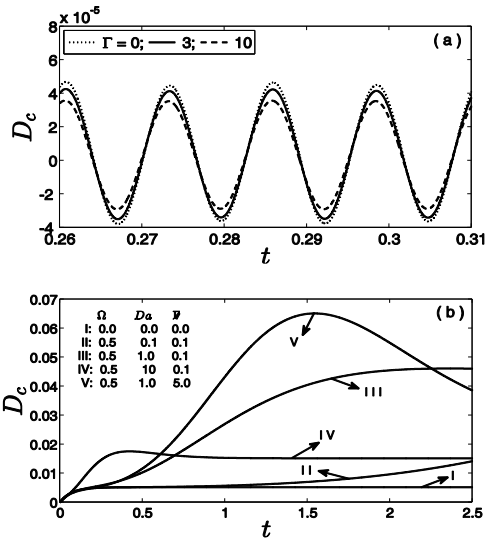

Fig. 3. (a) Plot of dispersion coefficient (D_c) with time for different values of absorption parameter (Γ) when $\gamma = Da = R_p = 0,$ and $\alpha = e = 0.5;$ (b) variation of D_c vs time under steady flow and unsteady convective diffusion when $\gamma = R_p = e = 0.$

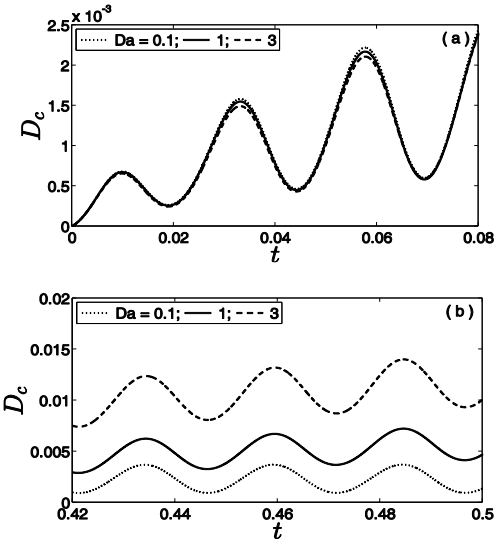

Fig. 4. Time variation of dispersion coefficient (D_c) for different values of Da when $\Gamma = 1$ in a two-fluid, three-layer Casson-Newtonian continuum $(\tau_y = 0.04, \gamma = 0.03)$. (a) For small times, and (b) for large times.

inferred that during the initial duration of time, D_c diminishes as the phase exchange rate increases;

since the increase in the value of Da is indicative of the increase in the reaction beyond the value of the rate of diffusion but the rate of decrease is not that significant. For instance at a fixed time 0.033, the computations of D_c, shown in Fig.4(a), are 0.001582, 0.001551 and 0.001494 respectively. From Fig. 4(b), one remarkable thing is seen, after a long time, D_c increases significantly with increase in the value of Da which is in keeping with the result of (Mazumder and Paul 2012). It is seen from Fig. 5(a), for small time, the values of D_c decrease as absorption increases whereas a variable effect of D_c is seen for the long time interval (Fig. 5(b)). The decrease of the D_c with an increase in the value of Γ is fully understandable in this case, as large Γ helps to enhance the irreversible chemical reaction rate. But due to the presence of high retention rate ($Da=1$) as compare to low irreversible reaction rate ($\Gamma=0.3$) at the boundary, a certain fall of D_c has been observed for larger time domain. Here, it is essential to note that the fall and growth of the dispersion coefficient with respect to the reaction parameters is not final. Based on the reaction strength, span of time, pipe radius, etc., the circumstances may change. Later, from Fig. 9, it has partially realized, though at the present moment we can predict that at long times the effect of the reversible reaction is more noticeable than that of the irreversible reaction.

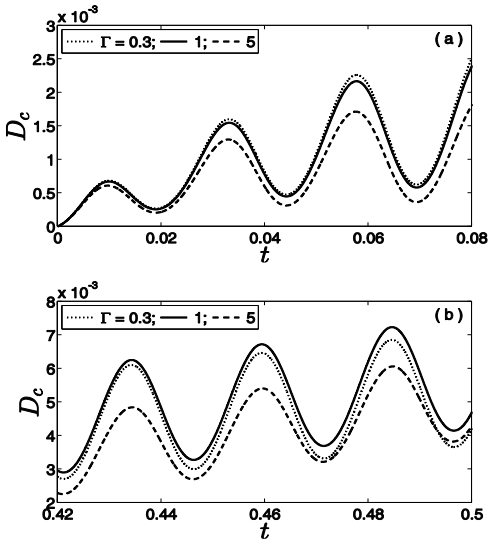

Fig. 5. Time variation of dispersion coefficient (D_c) for different values of Γ when $Da=1$ in a two-fluid, three-layer Casson-Newtonian continuum ($\tau_y=0.04, \gamma=0.03$). (a) For small times, and (b) for large times.

At low shear rate, the impact of yield stress is essentially significant while blood flows through small vessels or micro vessels. This aspect of a physiological context of the reliance of the dispersion coefficient on finite yield stress as well as peripheral layer thickness has been indicated in Figs. 6 and 7. Figs. 6 (a, b) show that with an increase in the value of yield stress a significant decrease in D_c follows at all times. This finding was also reported by Nagarani and Sebastian (2013), and Rana and Murthy (2016) they reasoned this to be due to the large velocity gradient at the boundary of pipe compared to that in the central region. We also obtained that the increase of peripheral layer thickness (γ) is to increase the magnitude of D_c (Figs. 7(a, b)). This happens because large values of γ signify larger Newtonian fluid region surrounding the central core Casson region, resulting in a larger value of D_c.

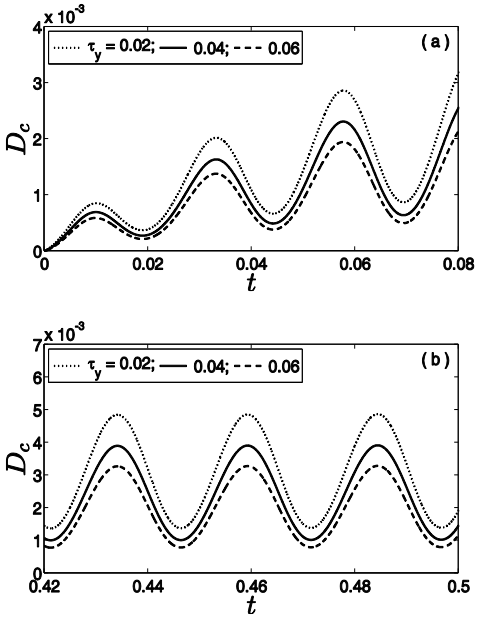

Fig. 6. Time variation of dispersion coefficient (D_c) for different values of yield stress (τ_y) when $\gamma=0.03, Da=0.1,$ and $\Gamma=0.3$.

The difference between the results of single-layer Newtonian fluid (i.e., τ_y = 0 and γ = 0), two-layer Casson fluid (i.e., $\tau_y=0.04$ and $\gamma=0$) and two-fluid, three-layer Casson-Newtonian continuum (i.e., $\tau_y=0.04$ and $\gamma=0.1$) is delineated in Fig. 8. Results of Figs. 8(a, b) reveal that the dispersion coefficient in the case of a single-layer Newtonian fluid is larger than that of the two-layer Casson model, a result that is in agreement with Dash, Jayaraman, and Mehta (2000). Further, the value of D_c of the two-fluid, three-layer Casson-Newtonian continuum is in between that of the single-layer Newtonian fluid and the two-layer Casson model, a physically meaningful result. The reason for the augmentation of the value of D_c due to the presence of the peripheral layer is that the Newtonian layer near the boundary has a larger velocity compared to that of the Casson layer and carries the effect of the chemical reaction at the boundary much faster in the

flow compared to that in the Casson fluid and thereby leading to a significant increase in the value of D_c.

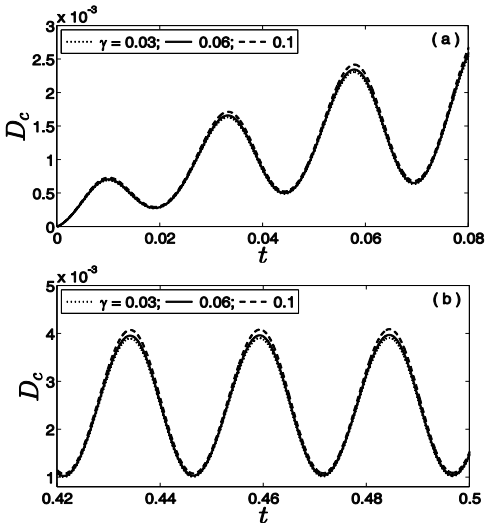

Fig. 7. Time variation of dispersion coefficient (D_c) for different values of peripheral layer thickness (γ) when $\tau_y = 0.04$, $Da = 0.1$ and $\Gamma = 0.3$.

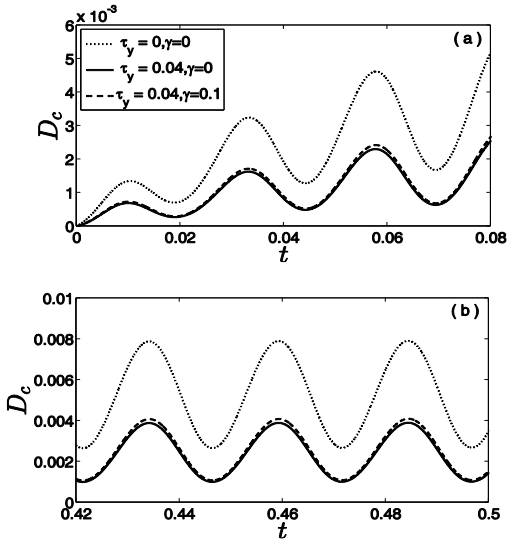

Fig. 8. Time variation of dispersion coefficient (D_c) for different fluid flow situations when $Da = 0.1$ and $\Gamma = 0.3$.

When the flow is steady (i.e., $e = 0$), dispersion coefficient as a function of Γ, for a static time ($t = 0.5$), is shown in Fig. 9(a) for the three chosen fluid models. It has seen, for small values of Γ (approximately 0.22 for the Newtonian fluid, 0.13 for Casson fluid and 0.12 for two-fluid, three-layer Casson-Newtonian continuum), dispersion coefficient increases and after a critical value of the dispersion coefficient it shows a steep decrease with absorption rate Γ. It is observed that for a three-layer fluid when $\Gamma = 100$, D_c decreases by 3.65 times of the value corresponding to $\Gamma = 0.01$, but for Casson and Newtonian fluids the decrements are 3.58 and 3.29 times respectively. Sankarasubramanian and Gill (1973) has already discussed this kind of result on D_c and we do not repeat this again here. At a fixed time $t = 5$, Fig. 9(b) points out a large increment to the value of D_c corresponding to small values of the retention parameter (Ω), but after a particular value of the parameter, it is monotonically decreasing. A Similar result was found and reasoned by Ng and Rudraiah (2008) which is true for this case also.

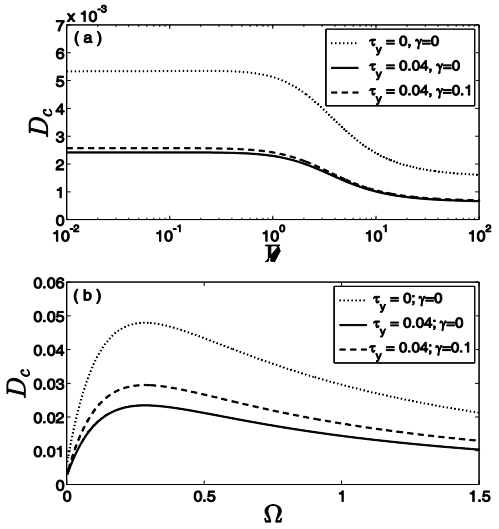

Fig. 9. Variation of dispersion coefficient with (a) Γ when $Da = 0$ at a fixed instant of time $t = 0.5$, and (b) Ω when $\Gamma = 0$ at a fixed instant of time $t = 5$.

The mean concentration distribution across the axial distance has been depicted in Figs. 10(a, c) and Figs. 10(b, d) at different instants of time, $t = 0.15$ and 0.5 respectively. It is found that peak of the mean concentration distribution translates significantly along the flow as reaction rates increase and also more importantly as time increases peaks get flat for large values of both the reaction parameter. Consequently, when the reaction rate is large enough, the long-time limit of the dispersion coefficient might not have a feasible implication.

CONCLUSION

The general conclusions that can be constructed from the present study are as follows:

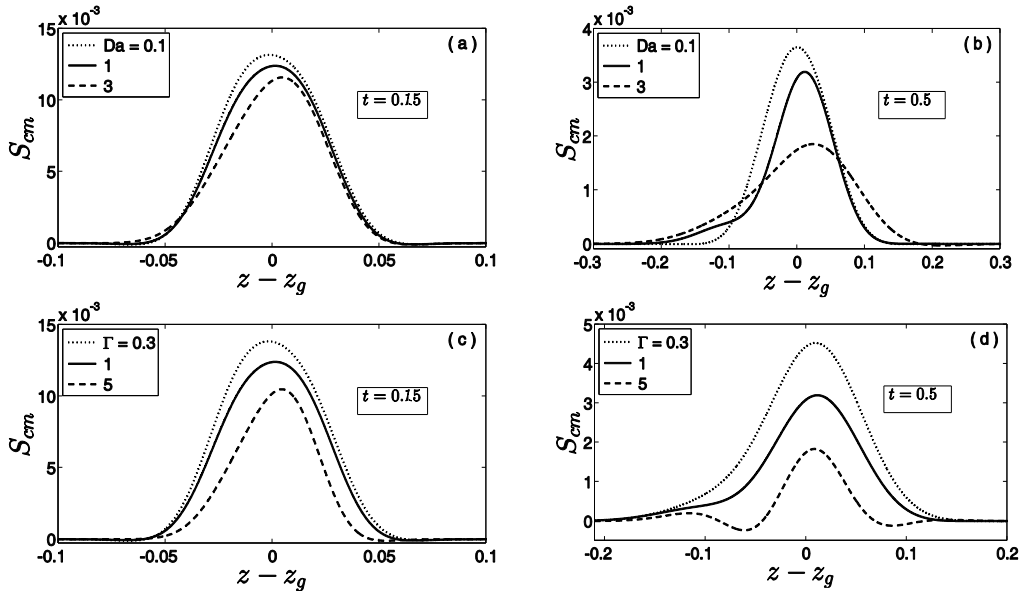

Fig. 10. Variation of mean concentration distribution (S_{cm})**, at a given instant** $t = 0.15$ **and** $t = 0.5$**. (a, b) For** Da **when** $\tau_y = 0.04, \gamma = 0.03, \Gamma = 1$**; and (c, d) for** Γ **when** $\tau_y = 0.04, \gamma = 0.03, Da = 1$.

(a) Increasing the value of the reversible reaction rate results in a decrease of D_c at the small time though D_c increases for the large time.

(b) An increase of irreversible reaction rate, dispersion coefficient decreases at small times.

(c) Due to high retention rate as of low absorption rate, an inconsistent nature of D_c is found for the large time.

(d) As yield stress increases the value of D_c decrease for all time.

(e) Larger the peripheral layer thickness, larger will be the D_c value.

(f) Because of peripheral layer presence, D_c in the three-layer Casson-Newtonian continuum to be larger than that in the two-layer Casson model but smaller than that of the single-layer Newtonian model.

(g) Dispersion coefficient is initially found to increase with small Γ, though as Γ increases the value of D_c decreases monotonically and ultimately reaches to its steady-state situation.

(h) For larger values of either Γ or Da lead to falling in the peak of the mean concentration profile and tends to become flat.

(i) The results obtained from this study has successfully satisfied with those of the existing works.

(j) The study in its present form has a significant impact on physiological blood flow analysis in comparison to various other work.

ACKNOWLEDGMENTS

Authors are thankful to the editor and reviewers for their constructive comments and suggestions, which has helped to improve this article. Mr. S. Debnath is grateful to National Institute of Technology, Agartala, India for providing financial assistance. We are thankful to Prof. B.S. Mazumder, ISI Kolkata, for the valuable suggestion to complete this work.

REFERENCES

Anderson, D., J. C. Tannehill, and R. H. Pletcher (1984). *Computational fluid mechanics and heat transfer*. Hemisphere Publishing Corporation, New York.

Aris, R. (1956). On the dispersion of a solute in a fluid flowing through a tube. *Proceedings of the Royal Society of London A: Mathematical, Physical and Engineering Sciences* 235(1200), 67–77.

Aroesty, J. and J. F. Gross (1972). The mathematics of pulsatile flow in small blood vessels: I. casson theory. *Microvascular research* 4(1), 1–12.

Balasubramanian, V., G. Jayaraman, and S. R. K. Iyengar (1997). Effect of secondary flows on contaminant dispersion with weak boundary absorption. *Applied Mathematical Modelling* 21(5), 275–285.

Barton, N. G. (1983). On the method of moments for

solute dispersion. *Journal of Fluid Mechanics* 126, 205–218.

Blair, G. W. S. (1959). An equation for the flow of blood, plasma and serum through glass capillaries. *Nature* 183(4661), 613–614.

Bugliarello, G. and J. Sevilla (1970). Velocity distribution and other characteristics of steady and pulsatile blood flow in fine glass tubes. *Biorheology* 7(2), 85–107.

Caro, C. G., T. J. Pedley, R. C. Schroter, and W. A. Seed (1978). *The mechanics of the circulation*. Oxford University Press.

Charm, S. and G. Kurland (1965). Viscometry of human blood for shear rates of 0-100,000 sec−1. *Nature* 206(4984), 617–618.

Cokelet, G. R. (1972). The rheology of human blood. In: Y. C. Fung (eds), *Biomechanics*, Prentice-Hall, Englewood Cliffs.

Dash, R. K., G. Jayaraman, and K. N. Mehta (2000). Shear augmented dispersion of a solute in a casson fluid flowing in a conduit. *Annals of Biomedical Engineering* 28(4), 373–385.

Davidson, M. R. and R. C. Schroter (1983). A theoretical model of absorption of gases by the bronchial wall. *Journal of Fluid Mechanics* 129, 313–335.

Debnath, S., S. Paul, and A. K. Roy (2018). Transport of reactive species in oscillatory annular flow. *Journal of Applied Fluid Mechanics* 11(2), 405–417.

Debnath, S., A. K. Saha, B. S. Mazumder, and A. K. Roy (2017a). Dispersion phenomena of reactive solute in a pulsatile flow of three-layer liquids. *Physics of Fluids* 29(9), 097107.

Debnath, S., A. K. Saha, B. S. Mazumder, and A. K. Roy (2017b). Hydrodynamic dispersion of reactive solute in a hagen-poiseuille flow of a layered liquid. *Chinese Journal of Chemical Engineering* 25(7), 862–873.

Debnath, S., A. K. Saha, and A. K. Roy (2017). A study on solute dispersion in a three layer blood-like liquid flowing through a rigid artery. *Periodica Polytechnica Mechanical Engineering* 61(3), 173–183.

Lau, M. W. and C. O. Ng (2007). On the early development of dispersion in flow through a tube with wall reactions. In: Zhuang F. G., Li J. C.(eds) *New Trends in Fluid Mechanics Research.* Springer, Berlin, Heidelberg.

Marŭsić-Paloka, E. and I. Păzanin (2011). On reactive solute transport through a curved pipe. *Applied mathematics letters* 24(6), 878–882.

Mazumder, B. S. and S. K. Das (1992). Effect of boundary reaction on solute dispersion in pulsatile flow through a tube. *Journal of Fluid Mechanics* 239, 523–549.

Mazumder, B. S. and K. K. Mondal (2005). On solute transport in oscillatory flow through an annular pipe with a reactive wall and its application to a catheterized artery. *The Quarterly Journal of Mechanics and Applied Mathematics* 58(3), 349–365.

Mazumder, B. S. and S. Paul (2012). Dispersion of reactive species with reversible and irreversible wall reactions. *Heat and Mass Transfer* 48(6), 933–944.

McDonald, D. A. (1974). *Blood flow in arteries*. Edward Arnold, London.

Mehta, R. V., R. L. Merson, and B. J. McCoy (1974). Hermite polynomial representation of chromatography elution curves. *Journal of Chromatography A* 88(1), 1–6.

Mondal, K. K. and B. S. Mazumder (2005). On solute dispersion in pulsatile flow through a channel with absorbing walls. International *Journal of Non-Linear Mechanics* 40(1), 69–81.

Nagarani, P., G. Sarojamma, and G. Jayaraman (2004). Effect of boundary absorption in dispersion in casson fluid flow in a tube. *Annals of Biomedical Engineering* 32(5), 706–719.

Nagarani, P. and B. T. Sebastian (2013). Dispersion of a solute in pulsatile non-Newtonian fluid flow through a tube. *Acta Mechanica* 224(3), 571–585.

Ng, C. O. (2006). Dispersion in steady and oscillatory flows through a tube with reversible and irreversible wall reactions. *Proceedings of the Royal Society of London A: Mathematical, Physical and Engineering Sciences* 462(2066), 481–515.

Ng, C. O. and N. Rudraiah (2008). Convective diffusion in steady flow through a tube with a retentive and absorptive wall. *Physics of Fluids* 20(7), 073604.

Paul, S. and B. S. Mazumder (2009). Transport of reactive solutes in unsteady annular flow subject to wall reactions. *European Journal of Mechanics-B/Fluids* 28(3), 411–419.

Păzanin, I. (2013). Modeling of solute dispersion in a circular pipe filled with micropolar fluid. *Mathematical and Computer Modelling* 57(9-10), 2366–2373.

Rana, J. and P. V. S. N. Murthy (2016). Solute dispersion in pulsatile casson fluid flow in a tube with wall absorption. *Journal of Fluid Mechanics* 793, 877–914.

Rosencrans, S. (1997). Taylor dispersion in curved channels. *SIAM Journal on Applied Mathematics* 57(5), 1216–1241.

Roy, A. K., A. K. Saha, and S. Debnath (2017). On dispersion in oscillatory annular flow driven jointly by pressure pulsation and wall oscillation. *Journal of Applied Fluid Mechanics* 10(5), 1487–1500.

Sankarasubramanian, R. and W. N. Gill (1973). Unsteady convective diffusion with interphase mass transfer. *Proceedings of the Royal Society of London A: Mathematical, Physical and Engineering Sciences* 333(1592), 115–132.

Sarkar, A. and G. Jayaraman (2004). The effect of wall absorption on dispersion in oscillatory flow in an annulus: application to a catheterized artery. *Acta Mechanica* 172(3-4), 151–167.

Sharp, M. K. (1993). Shear-augmented dispersion in non-Newtonian fluids. *Annals of Biomedical Engineering* 21(4), 407–415.

Siddheshwar, P. G. and S. Manjunath (2000). Unsteady convective diffusion with heterogeneous chemical reaction in a plane-poiseuille flow of a micropolar fluid. *International Journal of Engineering Science* 38(7), 765–783.

Siddheshwar, P. G. and S. Markande (1999). Unsteady convective diffusion of solute in a micropolar fluid flow through a cylindrical tube. *ZAMM-Journal of Applied Mathematics and Mechanics* 79(12), 821–833.

Taylor, G. I. (1953). Dispersion of soluble matter in solvent flowing slowly through a tube. *Proceedings of the Royal Society of London A: Mathematical, Physical and Engineering Sciences* 219(1137), 186–203.

Wu, Z. and G. Q. Chen (2014). Approach to transverse uniformity of concentration distribution of a solute in a solvent flowing along a straight pipe. *Journal of Fluid Mechanics* 740, 196–213.